THE JOURNAL OF PHYSICAL CHEMISTRY Letters

pubs.acs.org/JPCL Letter

Hole Transfer Promoted by a Viscosity Additive in an All-Polymer Photovoltaic Blend

Jianqiu Xu,[⊥] Rui Wang,[⊥] Shanshan Chen,[⊥] Chunfeng Zhang,* Lin Liu, Fengzhen Huang, Xiaomei Lu, Changduk Yang, Xiaoyong Wang, and Min Xiao

Cite This: *J. Phys. Chem. Lett.* 2020, 11, 1384−1389 Read Online

ACCESS | Metrics & More | Article Recommendations | Supporting Information

ABSTRACT: Viscosity modifiers are widely applied to improve the mechanical compliance of organic optoelectronic devices. However, the effect of the viscosity additives on the charge dynamics remains poorly understood. Here, we report the observation of markedly different effects of a high-viscosity polymeric additive on the electron- and hole-transfer dynamics in all-polymer organic photovoltaic blends. By using ultrafast transient absorption spectroscopy, we determine that hole transfer from charge-transfer excitations in the acceptor is markedly promoted while the electron transfer from local excitations in the donor remains nearly unchanged upon introduction of viscosity additives into the blends. We argue that the modification of dielectric screening is the mechanism underlying the effect of the additive on the charge dynamics. This finding suggests a new strategy for designing high-performance flexible organic photovoltaic devices by manipulating the dielectric environment.

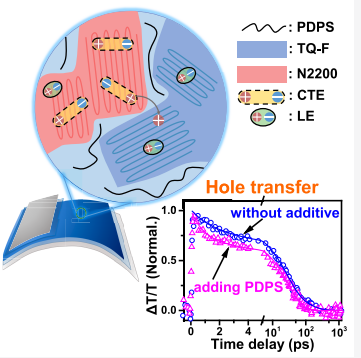

Downloaded via EAST CHINA NORMAL UNIV on September 22, 2020 at 06:19:12 (UTC).
See https://pubs.acs.org/sharingguidelines for options on how to legitimately share published articles.

Organic solar cells (OSCs) are promising candidates for power supplies in portable and wearable devices.[1−4] Benefiting from the stretchable mechanical properties of polymers, all-polymer OSCs, using polymers as both electron donors and acceptors, are particularly suitable for applications in flexible electronics.[5−9] An ideal OSC requires both efficient solar energy conversion and mechanical compliance.[10−12] Recently, remarkable progress has been achieved in improving the power conversion efficiencies (PCEs) of all-polymer solar cells.[13−18] Nevertheless, the efforts made to improve their mechanical compliance have been limited.[7]

To improve the mechanical ductility for photoactive layers or stretchable electrodes, viscosity modifiers have been widely employed in the fabrication of organic devices.[19−23] Unfortunately, the viscosity additives may cause severe declines in the electric properties of OSCs.[24−27] Recently, Chen et al. have made remarkable progress toward addressing the dilemma by introducing a high-viscosity processing polymer additive of poly(dimethylsiloxane-*co*-methyl phenethylsiloxane) (PDPS) into all-polymer OSCs.[20] The device performance has been dramatically improved with 90% PCE retained after 100 bending cycles.[20] However, the underlying mechanism, particularly how the viscosity additive affects the photocharge generation, remains unexplored.

Here, we report the observation of enhanced hole transfer by the viscosity additive (PDPS) in a model system of an all-polymer blend consisting of a polymer donor poly[6-fluoro-2,3-bis(3-octyloxyphenyl)quinoxaline-5,8-dyl-*alt*-thiophene-2,5-diyl] (TQ-F) and a naphthalene diimide-based polymer acceptor poly{[*N*,*N*′-bis(2-octyldodecyl)-naphthalene-1,4,5,8-bis(dicarboximide)-2,6-diyl]-*alt*-5,5′-(2,2′-bithiophene)} (N2200). By using ultrafast transient absorption (TA) spectroscopy, we systematically investigate the effect of the additive on the charge generation dynamics in the blend films with and without adding PDPS. When the viscosity additive is introduced into the blend, hole transfer becomes faster while electron transfer remains nearly unchanged. We ascribe these different effects of viscosity additives on the electron- and hole-transfer processes to the different dielectric screening on localized excitations in TQ-F and charge-transfer (CT) excitations in N2200, which is supported by characterization of the dielectric constants in the blend films with and without the PDPS additions. The findings in this work suggest the possibility of optimizing all-polymer OSCs by manipulating the dielectric screening in the photovoltaic blends.

The molecular structures and the absorption spectra of polymers studied in this work are shown in Figure 1. The polymer additive PDPS has no absorption in the visible to near-infrared wavelength range, suggesting that in both blends with or without the viscosity additive the solar energy is solely harvested by polymer donor TQ-F and acceptor N2200. Recently, the combination of TQ-F and N2200 has shown promising potential for applications as all-polymer devices using PDPS to improve mechanical flexibility. As reported in a

Received: January 3, 2020
Accepted: February 3, 2020
Published: February 3, 2020

ACS Publications © 2020 American Chemical Society

https://dx.doi.org/10.1021/acs.jpclett.0c00025
J. Phys. Chem. Lett. 2020, 11, 1384−1389

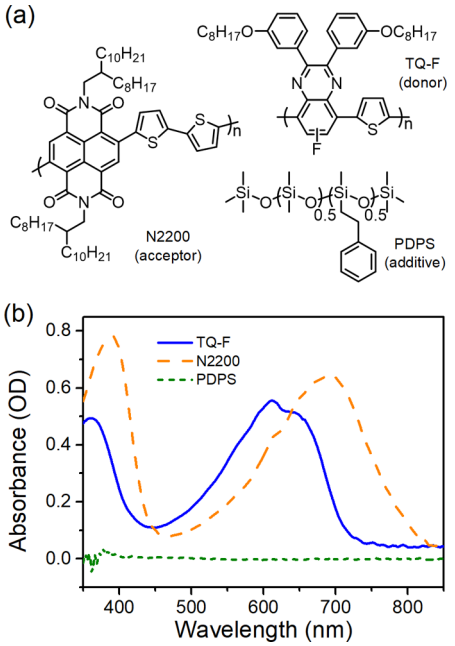

Figure 1. (a) Chemical structures of the polymer donor (TQ-F), acceptor (N2200), and additive (PDPS). (b) Absorption spectra of the polymers studied in this work.

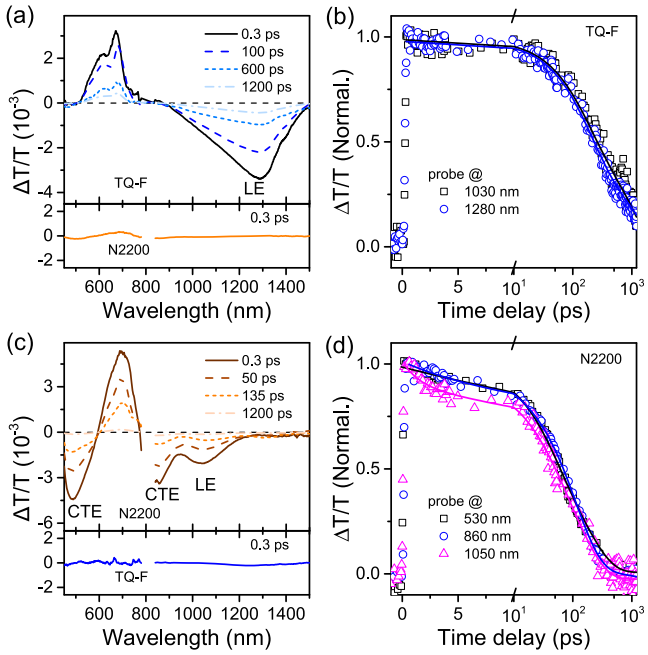

Figure 2. (a) TA spectra of the neat films of TQ-F (top) and N2200 (bottom) with pumping at 500 nm. (b) Normalized kinetic curves recorded from TQ-F reveal decay dynamics independent of the probe wavelength. (c) TA spectra of the neat films of N2200 (top) and TQ-F (bottom) with pumping at 740 nm. The ESA features of charge transfer and local excitations are labeled. (d) Normalized kinetic curves probed at different wavelengths. The probe wavelength-dependent decay dynamics of photoexcitation in N2200 indicates the coexistence of two excited features.

previous study, the performances of OSC devices are optimized with doping of 10 wt % PDPS in terms of PCEs and flexibility.[20] To study the effect of the viscosity additive on charge generation dynamics, we perform ultrafast TA spectroscopic measurements on the samples without and with the optimal PDPS additive (10% mass ratio). For TA measurements, the film samples are excited with wavelength-tunable pump pulses generated by an optical parametric amplifier (OperA Solo, Coherent) and probed with a white-light supercontinuum light beam covering the visible or near-infrared range. More experimental details are available in the Supporting Information.

In small organic molecules, Frenkel-type localized excitons are most widely generated upon optical excitation.[28−30] In addition, CT excitons may also be optically excited in conjugated polymers depending on the electron-withdrawing properties of the constituent units.[31−34] In the polymer donor TQ-F, the kinetics is nearly independent of the probe wavelength with pumping at 500 nm (Figure 2a,b), suggesting that the excited state is dominated by a single component of localized excitation. In the polymer acceptor of N2200, it is established that CT excitations (i.e., polaron pairs) are created together with localized excitations under photon illumination.[34] The coexistence of two types of excited states is manifested as different dynamics of excited-state absorption features. As established in our previous study,[34] the faster decay of the ESA feature at 1050 nm is related to the localized excitation, while the ESA bands at 530 and 860 nm with longer lifetimes are features of CT excitations (Figure 2d) with a weaker electron−hole interaction.[32] The spectral signature of CT excitations is confirmed by electrochemical absorption measurements.[34] It has been found that CT excitations rather than the local excitations in N2200 make the dominant contribution to the hole-transfer process in all-polymer blends.[34]

The dynamics of photocharge generation in OPV systems has been intensively studied in polymer/fullerene blends where electron transfer dominates the charge separation process. In all-polymer OPV blends, charge generation can be initiated by either electron-transfer or hole-transfer processes[34] because polymer acceptors absorb significantly in the visible to near-infrared wavelength range. For the TQ-F/N2200 blend, the electron-transfer process is triggered by local excitations in the donor TQ-F while the CT excitations in the acceptor of N2200 play a key role in the hole-transfer process.[34] We separately study the effects of viscosity additives on the electron- and hole-transfer processes by selectively exciting TQ-F at 500 nm and N2200 at 740 nm.

With pumping at 500 nm, the excitations in the blends are mainly induced by the absorption of the polymer donor (Figure 2). We observe a faster decay of the ESA feature at 1280 nm in the blends than in the neat TQ-F film, accompanied by increases in the intensities of the ESA signals at 860 and 1050 nm (Figure 3 and Figure S2). The electron transfer from donor TQ-F to acceptor N2200 is manifested with a spectral transfer in the TA data (Figure 3a and Figure S2). Because of electron transfer, the recombination of excited states in TQ-F (i.e., ESA at 1280 nm) becomes faster in the blends with respect to that in the neat donor film (Figure 3b), accompanied by increases in the intensities of the ESA signals at 860 and 1050 nm due to the formation of interfacial CT states (Figure 3a and Figure S2). The recombination lifetime of the early stage signal probed at 1280 nm is shortened from ∼260 ps in the neat TQ-F film to 5 ps in the blends with PDPS, suggesting that the electron transfer is highly efficient. Nonetheless, the decay dynamics of the ESA signal recorded

https://dx.doi.org/10.1021/acs.jpclett.0c00025
J. Phys. Chem. Lett. 2020, 11, 1384−1389

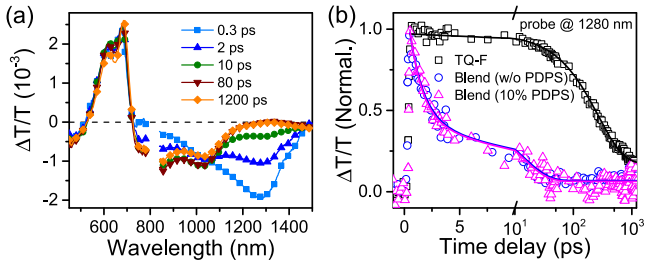

Figure 3. (a) TA spectra recorded from a blend film with 10% PDPS show the spectral evolution induced by electron transfer. (b) The faster decay of the ESA feature at 1280 nm in blends than in the TQ-F neat film reveals the electron-transfer process.

from the blends with and without PDPS additives is nearly the same (Figure 3b), implying that the effect of viscosity on the electron transfer induced by localized excitation is insignificant.

Figure 4 shows the TA data of hole-transfer dynamics in the blend film. Upon optical pumping at 740 nm, only polymer

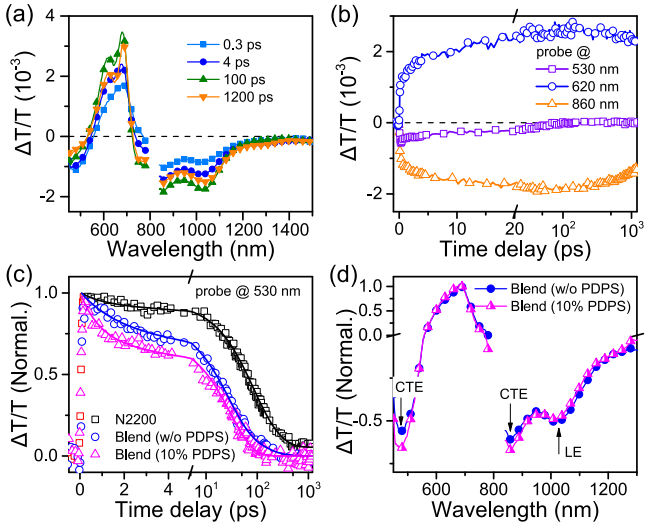

Figure 4. (a) TA spectra probed at various time delays and (b) kinetic curves probed at different wavelengths recorded for a blend film with 10% PDPS reveal the transfer of excitations from N2200 to TQ-F. (c) The ESA signal of N2200 at 530 nm decays much faster in blends than in the neat N2200 film. (d) Normalized TA spectra recorded at 0.3 ps from the blend films with and without the PDPS additive.

acceptor N2200 can be excited (Figure 2c). During the hole-transfer process, the intensity of the ESA feature at 530 nm gradually decreases while the intensities of the bleaching signal in the range of 580−710 nm and ESA features in the near-infrared range exhibit delay increases (Figure 4a,b). The delay increases in the visible range with two peaks, corresponding to the excited features from the neat TQ-F film (Figure 2a), can be assigned to the ground-state bleaching (GSB) signal of TQ-F caused by hole transfer. The resultant state exhibits enhanced ESA in the near-infrared range, which is entangled with the ESA signal of N2200 (Figure 4a). The signal probed in the visible band (<600 nm) may be contributed by both GSB of the donor and ESA of the interfacial CT state caused by hole transfer. The GSB and ESA signals are offset with similar amplitudes at 530 nm at the late stage after hole transfer. In this case, the time-dependent signal probed at 530 nm in the blend films represents the dynamics of CT excitation generated in N2200. To quantify the hole-transfer rate, we compare the dynamics at 530 nm measured from the blend and neat N2200 films (Figure 4c). The relaxation lifetime at the initial stage decreases in the blend films, suggesting the existence of a highly efficient hole-transfer process related to CT excitations. These spectral data of blend films can be reproduced well by global fitting analysis considering the localized or CT excitations in N2200 and the resultant interfacial charge-transfer state of hole transfer (Figure S4).

The effect of the PDPS additive on hole transfer is manifested with different relaxations of CT excitations in the blends with and without additives (Figure 4c). The early stage lifetimes are decreased from ∼100 ps in the neat N2200 film to ∼12 and ∼25 ps in the blends with and without additives, respectively, indicating that the hole-transfer process is much faster when the viscosity additive is introduced. Furthermore, the ESA features of CT excitons probed at 530 and 860 nm are enhanced in the blend with the additive if compared with that of local excitons, suggesting that the generation yields of CT excitations (i.e., polaron pairs) in the blends increase with the addition of PDPS (Figure 4d). These results suggest that the addition of PDPS not only promotes the generation of CT excitons but also improves the hole transfer induced by CT excitations, which is substantially different from the virtually unchanged electron transfer from TQ-F to N2200. In the all-polymer blends, the CT excitations instead of local excitations make the major contribution to hole transfer.[34] The enhancement of the generation of CT excitations and the promotion of hole transfer may compenetrate the side effects due to PDPS addition.

We discuss the possible mechanism underlying the different effects of the PDPS additive on the electron- and hole-transfer dynamics. Additives in polymer blends may affect the charge generation dynamics due to the change in the alignment and stacking of donors and acceptors as a consequence of morphology modification.[35−39] However, the morphological issue is unlikely to be the major factor underlying the additive effect on hole transfer in the blends. In our previous work, the differences in morphology and molecular packing are insignificant in the blends with and without additives as studied by GIWAXS,[20] which is consistent with the insignificant additive effect on the electron-transfer processes because the modification in morphology should simultaneously change the processes of electron and hole transfer.[36,40]

Next, we consider the effect of viscosity additive on the electronic response in the OPV blends. Unlike the evaporable solvent additives for morphological control, polymer additive PDPS remains in the blends after casting.[36] The incorporation of a third component such as this may change the dielectric screening of Coulomb interaction between electrons and holes in OPV blends,[41−45] which is plausibly responsible for the effect of the PDPS additive on the charge-transfer dynamics in the all-polymer blends. For further confirmation, we perform impedance and spectroscopic ellipsometry measurements to characterize the dielectric constant in different frequency regimes. The dielectric constant of the TQ-F/N2200 blend can be described as the mixture of TQ-F and N2200.[46,47] In the blend film with the PDPS additive, the dielectric constant shows a marked increase possibly due to the higher dielectric constant of PDPS (Figure 5). Considering the spatially separated nature of CT excitations, the increase in the dielectric constant results in a stronger screening effect, which decreases the binding energy of these electron−hole

https://dx.doi.org/10.1021/acs.jpclett.0c00025
J. Phys. Chem. Lett. 2020, 11, 1384−1389

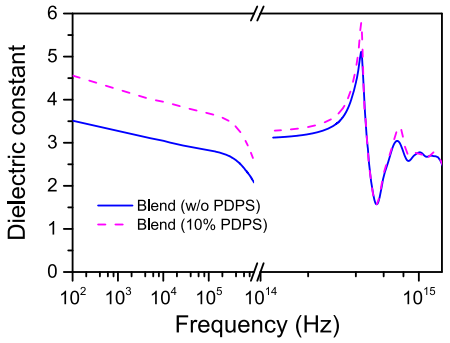

Figure 5. Dielectric constants with respect to frequency for blends without and with 10% PDPS. Adding the PDPS additive to the blend increases the film dielectric constant.

pairs and therefore favors hole transfer from N2200 to TQ-F.[43,48,49] However, for the tightly bound local excitations, the dynamics is less susceptible to the dielectric screening with an ultrashort electron−hole distance, as suggested in the literature.[50] Therefore, the increase in the dielectric constant may explain the different dependences on the viscosity additive for hole transfer related to CT excitations in acceptor N2200 and electron transfer related to local excitations in TQ-F.

In summary, we have shown that adding a viscosity additive induces faster hole transfer in TQ-F/N2200 blends in the pursuit of better mechanical compliance. We assign this promotion of hole transfer to the stronger dielectric screening effect on the charge-transfer excitations of N2200 after addition of the viscosity additive. Our results indicate the potential of polymeric additives in facilitating charge transfer by introducing favorable dielectric screening. Hence, further optimizations of viscosity additives relying on their intrinsic dielectric properties offer an effective approach for realizing practical flexible OSCs with good mechanical compliance along with good power conversion performance.

■ ASSOCIATED CONTENT

Supporting Information

The Supporting Information is available free of charge at https://pubs.acs.org/doi/10.1021/acs.jpclett.0c00025.

Experimental details, absorption and TA spectroscopic data of reference samples without a PDPS additive, low-frequency capacitance measurements, and spectroelectrochemistry data of TQ-F and N2200 (PDF)

■ AUTHOR INFORMATION

Corresponding Author

Chunfeng Zhang − *National Laboratory of Solid State Microstructures, School of Physics, and Collaborative Innovation Center for Advanced Microstructures, Nanjing University, Nanjing 210093, China;* orcid.org/0000-0001-9030-5606; Email: cfzhang@nju.edu.cn

Authors

Jianqiu Xu − *National Laboratory of Solid State Microstructures, School of Physics, and Collaborative Innovation Center for Advanced Microstructures, Nanjing University, Nanjing 210093, China*

Rui Wang − *National Laboratory of Solid State Microstructures, School of Physics, and Collaborative Innovation Center for Advanced Microstructures, Nanjing University, Nanjing 210093, China*

Shanshan Chen − *MOE Key Laboratory of Low-grade Energy Utilization Technologies and Systems, CQU-NUS Renewable Energy Materials & Devices Joint Laboratory, School of Energy & Power Engineering, Chongqing University, Chongqing 400044, China*

Lin Liu − *National Laboratory of Solid State Microstructures, School of Physics, and Collaborative Innovation Center for Advanced Microstructures, Nanjing University, Nanjing 210093, China*

Fengzhen Huang − *National Laboratory of Solid State Microstructures, School of Physics, and Collaborative Innovation Center for Advanced Microstructures, Nanjing University, Nanjing 210093, China*

Xiaomei Lu − *National Laboratory of Solid State Microstructures, School of Physics, and Collaborative Innovation Center for Advanced Microstructures, Nanjing University, Nanjing 210093, China;* orcid.org/0000-0002-8794-1000

Changduk Yang − *Department of Energy Engineering, School of Energy and Chemical Engineering, Perovtronics Research Center, Low Dimensional Carbon Materials Center, Ulsan National Institute of Science and Technology (UNIST), Ulsan 44919, South Korea;* orcid.org/0000-0001-7452-4681

Xiaoyong Wang − *National Laboratory of Solid State Microstructures, School of Physics, and Collaborative Innovation Center for Advanced Microstructures, Nanjing University, Nanjing 210093, China;* orcid.org/0000-0003-1147-0051

Min Xiao − *National Laboratory of Solid State Microstructures, School of Physics, and Collaborative Innovation Center for Advanced Microstructures, Nanjing University, Nanjing 210093, China; Department of Physics, University of Arkansas, Fayetteville, Arkansas 72701, United States*

Complete contact information is available at: https://pubs.acs.org/10.1021/acs.jpclett.0c00025

Author Contributions

⊥J.X., R.W., and S.C. contributed equally to this work.

Notes

The authors declare no competing financial interest.

■ ACKNOWLEDGMENTS

This work was supported by the National Key R&D Program of China (2018YFA0209100 and 2017YFA0303703), the National Natural Science Foundation of China (21922302, 21873047, 11574140, 91850105, 91833305, and 11904168), the Priority Academic Program Development of Jiangsu Higher Education Institutions (PAPD), and the Fundamental Research Funds for the Central Universities. C.Z. acknowledges financial support from Tang Scholar program.

■ REFERENCES

(1) Li, Y.; Xu, G.; Cui, C.; Li, Y. Flexible and semitransparent organic solar cells. *Adv. Energy Mater.* **2018**, *8*, 1701791.

(2) Qian, Y.; Zhang, X.; Xie, L.; Qi, D.; Chandran, B. K.; Chen, X.; Huang, W. Stretchable organic semiconductor devices. *Adv. Mater.* **2016**, *28* (42), 9243−9265.

(3) Lipomi, D. J.; Tee, B. C.; Vosgueritchian, M.; Bao, Z. Stretchable organic solar cells. *Adv. Mater.* **2011**, *23* (15), 1771−1775.

(4) Kaltenbrunner, M.; White, M. S.; Glowacki, E. D.; Sekitani, T.; Someya, T.; Sariciftci, N. S.; Bauer, S. Ultrathin and lightweight organic solar cells with high flexibility. *Nat. Commun.* **2012**, *3*, 770.

(5) Facchetti, A. Polymer donor−polymer acceptor (all-polymer) solar cells. *Mater. Today* **2013**, *16* (4), 123−132.
(6) Kim, T.; Kim, J. H.; Kang, T. E.; Lee, C.; Kang, H.; Shin, M.; Wang, C.; Ma, B.; Jeong, U.; Kim, T. S.; Kim, B. J. Flexible, highly efficient all-polymer solar cells. *Nat. Commun.* **2015**, *6*, 8547.
(7) Lee, C.; Lee, S.; Kim, G. U.; Lee, W.; Kim, B. J. Recent advances, design guidelines, and prospects of all-polymer solar cells. *Chem. Rev.* **2019**, *119* (13), 8028−8086.
(8) Genene, Z.; Mammo, W.; Wang, E.; Andersson, M. R. Recent advances in n-type polymers for all-polymer solar cells. *Adv. Mater.* **2019**, *31*, 1807275.
(9) Kim, W.; Choi, J.; Kim, J.-H.; Kim, T.; Lee, C.; Lee, S.; Kim, M.; Kim, B. J.; Kim, T.-S. Comparative study of the mechanical properties of all-polymer and fullerene−polymer solar cells: The importance of polymer acceptors for high fracture resistance. *Chem. Mater.* **2018**, *30* (6), 2102−2111.
(10) Park, S.; Heo, S. W.; Lee, W.; Inoue, D.; Jiang, Z.; Yu, K.; Jinno, H.; Hashizume, D.; Sekino, M.; Yokota, T.; Fukuda, K.; Tajima, K.; Someya, T. Self-powered ultra-flexible electronics via nano-grating-patterned organic photovoltaics. *Nature* **2018**, *561* (7724), 516−521.
(11) Lu, L.; Zheng, T.; Wu, Q.; Schneider, A. M.; Zhao, D.; Yu, L. Recent advances in bulk heterojunction polymer solar cells. *Chem. Rev.* **2015**, *115* (23), 12666−12731.
(12) Song, W.; Fan, X.; Xu, B.; Yan, F.; Cui, H.; Wei, Q.; Peng, R.; Hong, L.; Huang, J.; Ge, Z. All-solution-processed metal-oxide-free flexible organic solar cells with over 10% efficiency. *Adv. Mater.* **2018**, *30*, 1800075.
(13) Zhang, K.; Xia, R.; Fan, B.; Liu, X.; Wang, Z.; Dong, S.; Yip, H. L.; Ying, L.; Huang, F.; Cao, Y. 11.2% all-polymer tandem solar cells with simultaneously improved efficiency and stability. *Adv. Mater.* **2018**, *30*, 1803166.
(14) Wang, G.; Melkonyan, F. S.; Facchetti, A.; Marks, T. J. All-polymer solar cells: Recent progress, challenges, and prospects. *Angew. Chem., Int. Ed.* **2019**, *58* (13), 4129−4142.
(15) Li, Z.; Ying, L.; Zhu, P.; Zhong, W.; Li, N.; Liu, F.; Huang, F.; Cao, Y. A generic green solvent concept boosting the power conversion efficiency of all-polymer solar cells to 11%. *Energy Environ. Sci.* **2019**, *12* (1), 157−163.
(16) Fan, B.; Zhong, W.; Ying, L.; Zhang, D.; Li, M.; Lin, Y.; Xia, R.; Liu, F.; Yip, H. L.; Li, N.; Ma, Y.; Brabec, C. J.; Huang, F.; Cao, Y. Surpassing the 10% efficiency milestone for 1-cm(2) all-polymer solar cells. *Nat. Commun.* **2019**, *10*, 4100.
(17) Zhu, L.; Zhong, W.; Qiu, C.; Lyu, B.; Zhou, Z.; Zhang, M.; Song, J.; Xu, J.; Wang, J.; Ali, J.; Feng, W.; Shi, Z.; Gu, X.; Ying, L.; Zhang, Y.; Liu, F. Aggregation-induced multilength scaled morphology enabling 11.76% efficiency in all-polymer solar cells using printing fabrication. *Adv. Mater.* **2019**, *31*, 1902899.
(18) Yao, H.; Bai, F.; Hu, H.; Arunagiri, L.; Zhang, J.; Chen, Y.; Yu, H.; Chen, S.; Liu, T.; Lai, J. Y. L.; Zou, Y.; Ade, H.; Yan, H. Efficient All-Polymer Solar Cells based on a New Polymer Acceptor Achieving 10.3% Power Conversion Efficiency. *ACS Energy Lett.* **2019**, *4* (2), 417−422.
(19) Trung, T. Q.; Lee, N. E. Recent progress on stretchable electronic devices with intrinsically stretchable components. *Adv. Mater.* **2017**, *29*, 1603167.
(20) Chen, S.; Jung, S.; Cho, H. J.; Kim, N. H.; Jung, S.; Xu, J.; Oh, J.; Cho, Y.; Kim, H.; Lee, B.; An, Y.; Zhang, C.; Xiao, M.; Ki, H.; Zhang, Z. G.; Kim, J. Y.; Li, Y.; Park, H.; Yang, C. Highly flexible and efficient all-polymer solar cells with high-viscosity processing polymer additive toward potential of stretchable devices. *Angew. Chem., Int. Ed.* **2018**, *57* (40), 13277−13282.
(21) Kim, H.; Byun, J.; Bae, S.-H.; Ahmed, T.; Zhu, J.-X.; Kwon, S.-J.; Lee, Y.; Min, S.-Y.; Wolf, C.; Seo, H.-K.; Ahn, J.-H.; Lee, T.-W. On-fabrication solid-state N-doping of graphene by an electron-transporting metal oxide layer for efficient inverted organic solar cells. *Adv. Energy Mater.* **2016**, *6* (12), 1600172.
(22) Schroeder, B. C.; Chiu, Y.-C.; Gu, X.; Zhou, Y.; Xu, J.; Lopez, J.; Lu, C.; Toney, M. F.; Bao, Z. Non-conjugated flexible linkers in semiconducting polymers: A pathway to improved processability without compromising device performance. *Adv. Electron. Mater.* **2016**, *2*, 1600104.
(23) Lei, T.; Wang, J.-Y.; Pei, J. Roles of flexible chains in organic semiconducting materials. *Chem. Mater.* **2014**, *26* (1), 594−603.
(24) Kim, J.-S.; Kim, J.-H.; Lee, W.; Yu, H.; Kim, H. J.; Song, I.; Shin, M.; Oh, J. H.; Jeong, U.; Kim, T.-S.; Kim, B. J. Tuning mechanical and optoelectrical properties of poly(3-hexylthiophene) through systematic regioregularity control. *Macromolecules* **2015**, *48* (13), 4339−4346.
(25) Wang, G.-J. N.; Shaw, L.; Xu, J.; Kurosawa, T.; Schroeder, B. C.; Oh, J. Y.; Benight, S. J.; Bao, Z. Inducing elasticity through oligosiloxane crosslinks for intrinsically stretchable semiconducting polymers. *Adv. Funct. Mater.* **2016**, *26* (40), 7254−7262.
(26) Savagatrup, S.; Makaram, A. S.; Burke, D. J.; Lipomi, D. J. Mechanical properties of conjugated polymers and polymer-fullerene composites as a function of molecular structure. *Adv. Funct. Mater.* **2014**, *24* (8), 1169−1181.
(27) Printz, A. D.; Lipomi, D. J. Competition between deformability and charge transport in semiconducting polymers for flexible and stretchable electronics. *Appl. Phys. Rev.* **2016**, *3* (2), 021302.
(28) Clarke, T. M.; Durrant, J. R. Charge photogeneration in organic solar cells. *Chem. Rev.* **2010**, *110*, 6736−6767.
(29) Hou, J.; Inganas, O.; Friend, R. H.; Gao, F. Organic solar cells based on non-fullerene acceptors. *Nat. Mater.* **2018**, *17* (2), 119−128.
(30) Coropceanu, V.; Chen, X.-K.; Wang, T.; Zheng, Z.; Brédas, J.-L. Charge-transfer electronic states in organic solar cells. *Nat. Rev. Mater.* **2019**, *4* (11), 689−707.
(31) Niu, M. S.; Wang, K. W.; Yang, X. Y.; Bi, P. Q.; Zhang, K. N.; Feng, X. J.; Chen, F.; Qin, W.; Xia, J. L.; Hao, X. T. Hole transfer originating from weakly bound exciton dissociation in acceptor-donor-acceptor nonfullerene organic solar cells. *J. Phys. Chem. Lett.* **2019**, *10* (22), 7100−7106.
(32) Tautz, R.; Da Como, E.; Limmer, T.; Feldmann, J.; Egelhaaf, H. J.; von Hauff, E.; Lemaur, V.; Beljonne, D.; Yilmaz, S.; Dumsch, I.; Allard, S.; Scherf, U. Structural correlations in the generation of polaron pairs in low-bandgap polymers for photovoltaics. *Nat. Commun.* **2012**, *3*, 970.
(33) Tautz, R.; Da Como, E.; Wiebeler, C.; Soavi, G.; Dumsch, I.; Frohlich, N.; Grancini, G.; Allard, S.; Scherf, U.; Cerullo, G.; Schumacher, S.; Feldmann, J. Charge photogeneration in donor-acceptor conjugated materials: influence of excess excitation energy and chain length. *J. Am. Chem. Soc.* **2013**, *135* (11), 4282−4290.
(34) Wang, R.; Yao, Y.; Zhang, C.; Zhang, Y.; Bin, H.; Xue, L.; Zhang, Z.-G.; Xie, X.; Ma, H.; Wang, X.; Li, Y.; Xiao, M. Ultrafast hole transfer mediated by polaron pairs in all-polymer photovoltaic blends. *Nat. Commun.* **2019**, *10*, 398.
(35) Lou, S. J.; Szarko, J. M.; Xu, T.; Yu, L.; Marks, T. J.; Chen, L. X. Effects of additives on the morphology of solution phase aggregates formed by active layer components of high-efficiency organic solar cells. *J. Am. Chem. Soc.* **2011**, *133* (51), 20661−20663.
(36) McDowell, C.; Abdelsamie, M.; Toney, M. F.; Bazan, G. C. Solvent additives: Key morphology-directing agents for solution-processed organic solar cells. *Adv. Mater.* **2018**, *30*, 1707114.
(37) Liao, H.-C.; Ho, C.-C.; Chang, C.-Y.; Jao, M.-H.; Darling, S. B.; Su, W.-F. Additives for morphology control in high-efficiency organic solar cells. *Mater. Today* **2013**, *16* (9), 326−336.
(38) Schmidt, K.; Tassone, C. J.; Niskala, J. R.; Yiu, A. T.; Lee, O. P.; Weiss, T. M.; Wang, C.; Frechet, J. M.; Beaujuge, P. M.; Toney, M. F. A mechanistic understanding of processing additive-induced efficiency enhancement in bulk heterojunction organic solar cells. *Adv. Mater.* **2014**, *26* (2), 300−305.
(39) Zhao, J.; Li, Y.; Yang, G.; Jiang, K.; Lin, H.; Ade, H.; Ma, W.; Yan, H. Efficient organic solar cells processed from hydrocarbon solvents. *Nat. Energy* **2016**, *1* (2), 15027.
(40) Kyaw, A. K. K.; Wang, D. H.; Luo, C.; Cao, Y.; Nguyen, T.-Q.; Bazan, G. C.; Heeger, A. J. Effects of solvent additives on morphology, charge generation, transport, and recombination in solution-processed small-molecule solar cells. *Adv. Energy Mater.* **2014**, *4* (7), 1301469.

https://dx.doi.org/10.1021/acs.jpclett.0c00025
J. Phys. Chem. Lett. 2020, 11, 1384−1389

(41) Nalwa, K. S.; Carr, J. A.; Mahadevapuram, R. C.; Kodali, H. K.; Bose, S.; Chen, Y.; Petrich, J. W.; Ganapathysubramanian, B.; Chaudhary, S. Enhanced charge separation in organic photovoltaic films doped with ferroelectric dipoles. *Energy Environ. Sci.* **2012**, *5* (5), 7042−7049.
(42) Chen, B.; Zhang, W.; Zhou, X.; Huang, X.; Zhao, X.; Wang, H.; Liu, M.; Lu, Y.; Yang, S. Surface plasmon enhancement of polymer solar cells by penetrating Au/SiO2 core/shell nanoparticles into all organic layers. *Nano Energy* **2013**, *2* (5), 906−915.
(43) Leblebici, S.; Lee, J.; Weber-Bargioni, A.; Ma, B. Dielectric screening to reduce charge transfer state binding energy in organic bulk heterojunction photovoltaics. *J. Phys. Chem. C* **2017**, *121* (6), 3279−3285.
(44) Clarke, T. M.; Durrant, J. R. Charge photogeneration in organic solar cells. *Chem. Rev.* **2010**, *110* (11), 6736−6767.
(45) Donaghey, J. E.; Armin, A.; Burn, P. L.; Meredith, P. Dielectric constant enhancement of non-fullerene acceptors via side-chain modification. *Chem. Commun.* **2015**, *51* (74), 14115−14118.
(46) Lu, Y.; Xiao, Z.; Yuan, Y.; Wu, H.; An, Z.; Hou, Y.; Gao, C.; Huang, J. Fluorine substituted thiophene-quinoxaline copolymer to reduce the HOMO level and increase the dielectric constant for high open-circuit voltage organic solar cells. *J. Mater. Chem. C* **2013**, *1* (4), 630−637.
(47) Xu, X.; Li, Z.; Wang, J.; Lin, B.; Ma, W.; Xia, Y.; Andersson, M. R.; Janssen, R. A. J.; Wang, E. High-performance all-polymer solar cells based on fluorinated naphthalene diimide acceptor polymers with fine-tuned crystallinity and enhanced dielectric constants. *Nano Energy* **2018**, *45*, 368−379.
(48) Sami, S.; Haase, P. A. B.; Alessandri, R.; Broer, R.; Havenith, R. W. A. Can the dielectric constant of fullerene derivatives be enhanced by side-chain manipulation? A predictive first-principles computational study. *J. Phys. Chem. A* **2018**, *122* (15), 3919−3926.
(49) de Gier, H. D.; Jahani, F.; Broer, R.; Hummelen, J. C.; Havenith, R. W. Promising strategy to improve charge separation in organic photovoltaics: Installing permanent dipoles in PCBM analogues. *J. Phys. Chem. A* **2016**, *120* (27), 4664−4671.
(50) van Duijnen, P. T.; de Gier, H. D.; Broer, R.; Havenith, R. W. A. The behaviour of charge distributions in dielectric media. *Chem. Phys. Lett.* **2014**, *615*, 83−88.

https://dx.doi.org/10.1021/acs.jpclett.0c00025
J. Phys. Chem. Lett. 2020, 11, 1384−1389